Buckling of Short Cylinders with Elliptical Head and Core Support Structure Under Transverse Shearing Loads

T. Murakami, H. Yoguchi, H. Hirayama
Toshiba Corporation, Yokohama, Japan
Y. Sawada, H. Nakamura
Central Research Institute of Electric Power Industry, Abiko, Japan

Introduction

Following the technical assessment study of a pool-type LMFBR in Japan located in an earthquake prone zone(1984-1986), a demonstration test and research program(1987-1993) sponsered by the Ministry of International Trade and Industry (MITI) is being made by Central Research Institute of Electric Power Industry (CRIEPI) in cooperation with Toshiba Corp., Hitachi Ltd., Mitsubishi Heavy Industries, Ltd. and Kawasaki Heavy Industries, Ltd. As a theme of this program buckling is considered to be one of the most important subjects to improve the reliability and reduce the construction cost for a demonstration fast breeder reactor in Japan. In these studies(Sawada 1989, Nakamura 1987, Matsuura 1989, Murakami 1987, Kokubo 1987, Nakagawa 1989, Kawamoto 1987 and 1989), buckling tests and analyses were performed to clarify the basic buckling characteristics for short cylinders and core support structures and direct to establish the rational design method. For a short cylinder, wherein the shear buckling might occure, Lundquist(1935) and Yamaki(1980) carried out elastic buckling tests . Some related tests with plastic shear buckling were made by Galletly (1985), Akiyama(1987) and authors mentioned above. However these tests were made using cylinders with heavy flanges on both ends, therefore, it is needed to investigate the end boundary condition having a head at one end of the cylinders where it would arise in the practice of a pool-type LMFBR main vessel. In this paper, as one of the themes of this program, buckling tests were carried out using four models with heads on one end of the cylinders and two commonly used cylinders. The end effects on the buckling load and post buckling behavior were clarified and the prediction of the buckling load were examined.

Buckling test setup and models

The purpose of this study is to investigate the end effects caused by a head on the buckling characteristics of short cylindrical shells as described before. Consequently it is needed to apply a transverse shearing load directly to the core support structures. The loading-lever, supported on a base plate as shown in Fig.1, transmitted a shearing load caused by a hydraulic actuator to test models with heads on one end. The shearing force was applied at a point of 600 mm apart from the fixed end of test models, and hence the bending-to-shearing stress ratio was 1.2 in these tests. As shown in Table 1., six models, having 1000mm diameter and radius-to-thickness ratio R/t=167 and 250, were prepared. Four models(CO-167-1,-2,CO-250-1,-2) were with 2:1 elliptical heads on one end of the cylindrical shells. On the other hand, the remaining two models(CY-167, CY-250), cylindrical shells with heavy flanges on both ends, were also tested in the same manner to verify the testing method described above and as reference data examining the effects of boundary conditions caused by the head. These models were fabricated by rolling the stainless steel plates with one welded seam along the longitudinal direction. The elliptical heads were fabricated by a hydraulic press and welded together at one end of the cylindrical shells with the core support structures. The other end of these cylinders were fixed to flanges with bands and welding. The configuration of these models are shown in Fig.2. Initial shape imperfections were measured for each model at 5 (CY-167,CY-250) and 6(CO-167,CO-250) longitudinal cross sections. In the former models the maximum shape deviation occured at the center, but, in the latter models, it gradually increased along the longitudinal direction and attained the maximum value at the end of cylindrical shells where heads were welded. The example of measured imperfections are shown in Fig.3. The maximum values were almost within 1mm, except for models CO-250, where weld deformation were induced because of the thin thickness of the plate.

Numerical analysis

Calculations were carried out with the general-purpose finite element analysis code MARC. Analysis models, 180° sector models taking advantage of symmetry, for a cylinder without a head and a cylinder with a head and the core support structures are shown in Fig.4 using the doubly-curved thin shell elements(Element 4). For cylindrical shells, the number of elements in circumferential and axial directions were 18 and 8, respectively. The distributions of 0.2% proof stress were observed in the head part caused by press work. Hence, these were correctly modeled using measured data with small test pieces cut out from the head. Forced displacements were applied at the illustrated points in the figure. The stress-strain curves measured were modeled by piecewise linear relations and imperfections measured were also modeled using the Fourier series expansions considering the first 15 terms.

Results and discussion

(1)Load-displacement curves

Typical load-displacement relations are shown in Fig.5 and Fig.6, where displacements were evaluated at the cylinder ends. In these figures, it was observed that the buckling loads(the maximum loads governed by the shear mode in this paper) decreased slightly for CO-167 and CO-250 compared with those for CY-167 and CY-250. These load reduction ratios were rather high for increasing radius-to-thickness ratio. In these figures, wherein the shear buckling exhibited very stable behavior, the load-displacement curves for CO-167 and CO-250 showed rather steep load decreases in the post buckling region. Load-displacement curves for CO-167 under cyclic loads are shown in Fig.7. It was clarified that the buckling load in the first reverse direction was nearly equal to the former one and successive load-displacement relations were similar to those of commonly used cylinders. Buckling loads for these models are summarized in Table 2.

(2)Buckling mode

Typical buckling modes for CY-250 and CO-250 measured at every 10mm distance along the longitudinal direction are shown in Fig.8. For the cylinder(CY-250), buckling wrinkles were nearly equal to zero at both ends. On the contrary, for the cylinders with heads(CO-250), small wrinkles were found at one end of x/L=1.0. For more precise understandings, the amplitude of those wrinkles, evaluated at the specified wave exhibiting the maximum value, are also shown in Fig. 8. It was observed that the peak position of wrinkles shifted to about 40-50mm towards the head direction and it was caused by a lack of in-plane rigidity at this end compared with the cylinder having rigid flanges at both ends. This shift was also verified by the numerical analysis for these two models and the distributions of buckling wrinkles agreed well as shown in Fig.9.

(3)Estimation of buckling loads

Using the theoretical torsional buckling stress given in Eq.(1), the ϕ-method, whereby the plastic buckling loads were evaluated using the quadratic interaction relation with the yield stress, was examined.

$$\tau_{el}=C_t Et/R \qquad C_t=4.83(1+0.0239(L/\sqrt{Rt})^3)^{0.5}/(L/\sqrt{Rt})^2 \tag{1}$$

$$\frac{1}{\tau_p^2}=\frac{1}{\tau_{el}^2}+\frac{1}{\tau_y^2} \qquad \text{or} \qquad \frac{1}{Q_p^2}=\frac{1}{Q_{el}^2}+\frac{1}{Q_y^2} \tag{2}$$

where τ_y :shear yield stress $\quad$ τ_p :plastic shear buckling stress
$\qquad$ Qy :shear yield load ($\pi Rt\tau_y$) $\quad$ Qp :plastic shear bucklind load ($\pi Rt\tau_p$)

The buckling loads tested Qexp normalized to the shear yield loads Qy are plotted in Fig.10 with the curve obtained by Eqs.(1) and (2) using the plasticity parameter given in Eq.(3)

$$\lambda = \sigma_y / E \frac{t}{R} \tag{3}$$

The buckling loads for cylinders(CY-167,CY-250) were in good agreement with those obtained by the ϕ-method. For cylinders with heads(CO-167,CO-250), test results were a little lower. The values of 0.97 for CO-167 and 0.87 for CO-250 were obtained compared with those by the ϕ-method prediction. In Fig.11, the buckling loads for cylinders with heads normalized to those without heads are also shown along R/t.

(4)Effect of the head on buckling loads

In some pressure vessel design code(ASME code) under external pressure, it is recommended to use the equivalent length adding one-third of the head depth to the cylinder to guarantee the fixed boundary condition at this point. In this study the additional length was 83mm, which was considered to be the conservative estimation of the peak point shift indicated in Figs.8 and 9. Using this equivalent length, the predicted curves are also shown in Figs.10 and 11. This value approached to 1.0 for small values of λ and R/t, where the plastic buckling were dominant, and in the elastic buckling range the discrepancy was 7.5% at most. The predicted values were in good agreement for CO-167. But, test results for CO-250 showed rather lower buckling loads caused by larger initial imperfections for these models as indicated in Fig.3. To confirm the effect of these imperfections, numerical analyses were carried out with measured imperfections as shown in Fig.11, where better agreement was obtained. When designing the main vessel in a fast breeder reactor(LMFBR), it was most severe in the operating condition under the seismic transverse shearing loads. In these circumstances, the plasticity parameter was below 0.2 in Fig.10 because of the decreasing yield stress, hence, the buckling loads with the heads were considered to be almost the same as those for the cylinders.

Conclusions

Regarding to the end effects caused by a head on the buckling characteristics, the following results were obtained from model tests and numerical analyses wherein cylinders with heads were loaded through the core support structures.

1. The shear buckling loads decreased slightly for cylinders with heads compared with those for cylinders without heads. These reduction ratios were rather high for larger values of R/t.
2. Peak position of the buckling wrinkles moved to about 40-50mm towards the head direction caused by a lack of in-plane rigidity at this end compared with the cylinders having heavy flanges at both ends. This shift was also verified by the numerical analysis for these two models.
3. The buckling loads for cylinders were in good agreement with the ϕ-method predictions. Applying the equivalent length adding one-third of the head

depth to the cylinder, considered to be the conservative estimation, the predictions were in good agreement with test results for CO-167.

4. In the operating temperature of a main vessel, because of the increasing plasticity, the buckling loads with heads were considered to be almost the same as those for the cylinders.

Acknowledgement

The authors gratefully acknowledge the helpful discussion of Prof. H. Akiyama, Prof. H. Otsubo (University of Tokyo) and members of the Buckling Subcommittee throughout the course of this work.

References

Sawada, Y. et al (1989). Demonstration Test and Research Program of Buckling of FBR. to be presented at 10th SMiRT

Nakamura, H. et al (1987). Plastic Buckling of Short Cylinders with Axial Temperature Distribution under Transverse Shearing Loads. 9th SMiRT E4/9

Matsuura, H. et al (1989). Shear Buckling of 304SS Cylinders Having Radius-to-Thickness Ratio of 100 thru 400 under Transverse Shearing Loads. to be presented at 10th SMiRT

Murakami, T. et al (1987). Buckling Strength of Elliptical Heads with Core Support Structure under Vertical and Horizontal Loads. 9th SMiRT E4/4

Kokubo, K. et al (1987). Buckling Behaviors of Short Cylindrical Shells under Dynamic Loads. 9th SMiRT E4/2

Nakagawa, M. et al (1989). Post Buckling Behavior of the Short Cylindrical Shells under Lateral Seismic Loads. to be presented at 10th SMiRT

Kawamoto, Y. et al (1987). Plastic Buckling of Short Cylinders under Transverse Shearing Loads. 9th SMiRT E4/10

Kawamoto, Y. et al (1989). The Effect of Thermal Loads on the Buckling Strength of a Fast Breeder Reactor Vessel. to be presented at 10th SMiRT

Lundquist. E.E. (1935). Strength tests of Thin-walled Duralumin Cylinders in Combined Transverse Shear and Bending. NACA TN-523

Yamaki. N. et al (1980). Buckling of Circular Cylindrical Shells under Combined Action of Transverse Edge Load and Hydrostatic Pressure. Thin-walled Structures, pp. 286-298(Granada Pub.)

Galletly, G.D. et al (1985). Plastic Buckling of Short Vertical Cylindrical Shells Subjected to Horizontal Edge Shear Loads. J. of Pressure Vessel Technology, Vol. 107, pp. 101-106

Akiyama, H. (1987). Buckling Tests of Steel Cylindrical Shells Subjected to Combined Bending and Shear(in Japanese). J. of Structural and Construction Engineering, Vol. 371, pp. 44-51

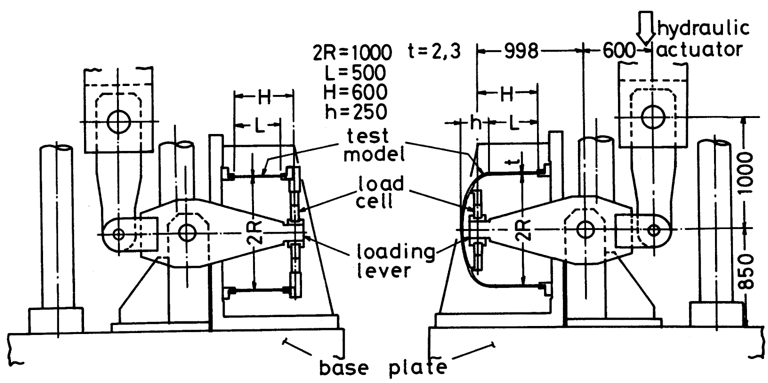

Fig.1 Test setup for cylinders with and without heads

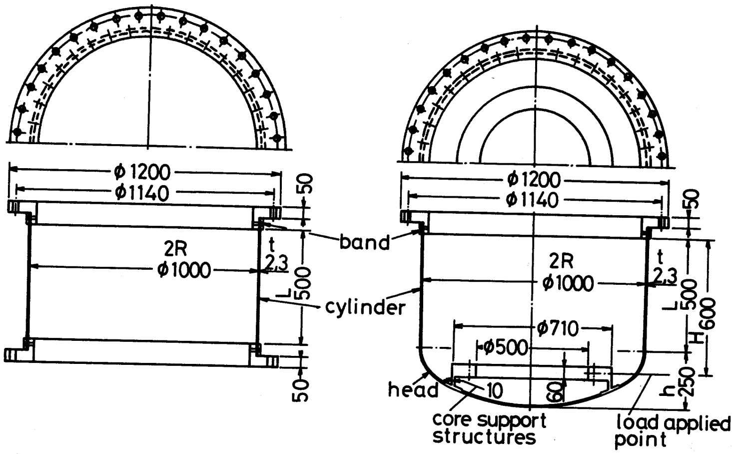

Fig.2 Configuration of test models with and without heads

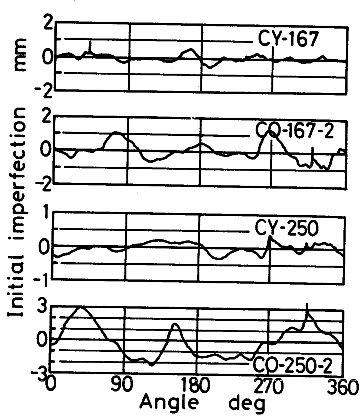

Fig.3 Measured initial imperfections

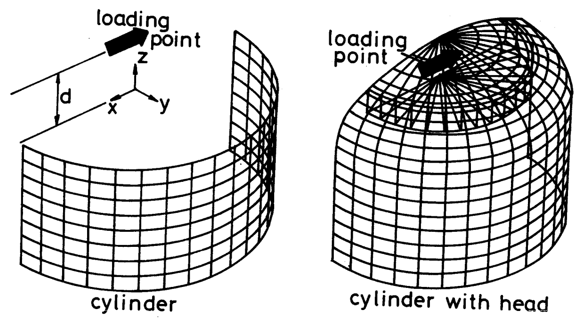

Fig.4 Finite element models

Table 1. Geometric and physical properties for test models

Test model	R mm	t mm	L mm	H mm	E kgf/mm²	σ_y kgf/mm²
CY-167	500	3.04	500	600	1.93x10⁴	32.5
CO-167-1						
CO-167-2						
CY-250	500	1.97	500	600	1.93x10⁴	30.6
CO-250-1						
CO-250-2						

CY··· cylinder CO···cylinder with head

Table 2. Experimental buckling loads and theoretical predictions

Test model	Q_{exp} ton	Q_{el} ton	Q_y ton	Q_ϕ ton	Q_{exp}/Q_y	Q_{exp}/Q_ϕ
CY-167	71.0	118	89.6	71.3	0.793	0.996
CO-167-1	70.3				0.784	0.986
CO-167-2	68.3				0.762	0.958
CY-250	33.6	44.3	54.7	34.4	0.615	0.977
CO-250-1	30.4				0.556	0.883
CO-250-2	29.5				0.539	0.858

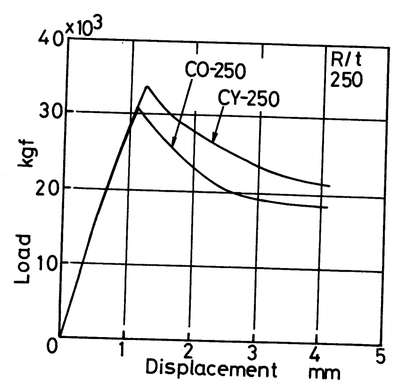

Fig.5 Comparison of load-displacement curves for R/t=250

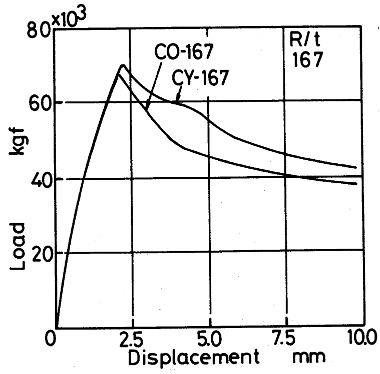

Fig.6 Comparison of load-displacement curves for R/t=167

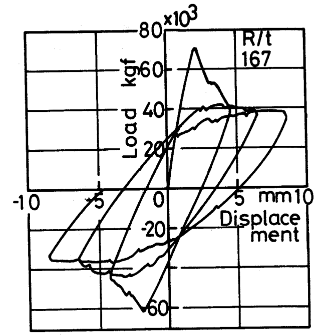

Fig.7 Cyclic load-displacement curve for R/t=167

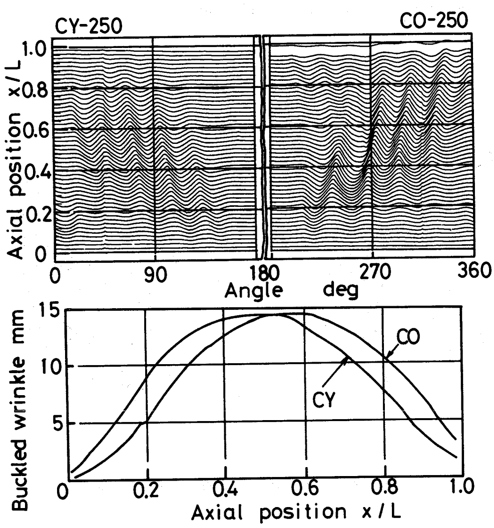

Fig.8 Distributions of measured buckling mode

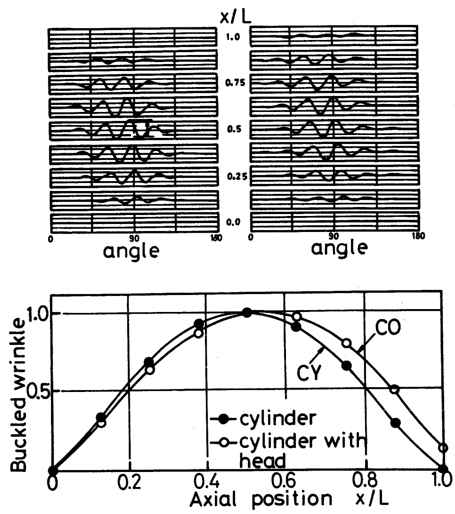

Fig.9 Distributions of calculated buckling mode

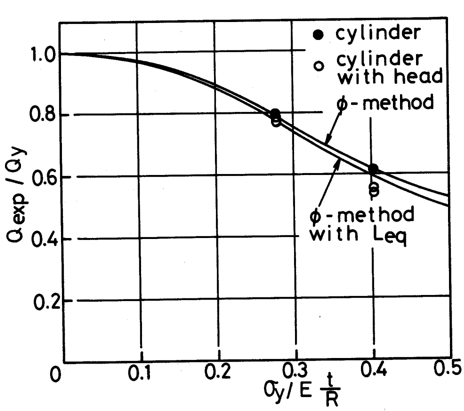

Fig.10 Comparison of buckling loads for cylinders with and without heads

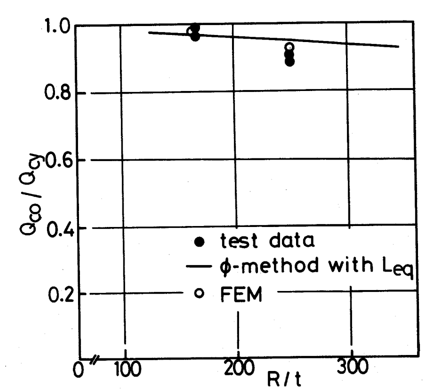

Fig.11 Reduction ratio of Buckling loads for cylinders with heads